3-D ideal MHD stability of super dense core plasma in LHD

Y. Narushima, K.Y. Watanabe, R. Sakamoto, Y. Suzuki, S. Sakakibara, S. Ohdachi,
H. Yamada and LHD experimental group
W.A. Cooper[a]

National Institute for Fusion Science, 322-6 Oroshi-cho, Toki 509-5292, Japan
[a] Centre de Recherches en Physique des Plasmas,
Association Euratom / Confederation Suisse, EPFL, 1015 Lausanne, Switzerland

The characteristics of confinement properties and magnetohydrodynamics (MHD) stabilities of the super dense core (SDC) plasmas are intensively studied in the Large Helical Device (LHD) experiment. The SDC plasmas are produced in the configuration with outward shifted magnetic axis and rapid fueling into the core region by pellet injection. The SDC plasmas have high electron pressure due to the large electron density (n_e~10^{21}[m^{-3}]) in the core region which induces a large Shafranov shift (Δ/a_{eff}>0.5). It is useful to apply the production method of the SDC plasmas for obtaining high-beta plasmas with high pressure in the core region. In this study, the characteristics of the ideal MHD instabilities of the SDC plasmas are analyzed by using the 3-D ideal MHD code TERPSICHORE. The calculated equilibrium of the typical SDC plasma with the central beta of β_0 = 5[%] solved as the result of the HINT/HINT2 codes shows that a deep magnetic well depth appears around the core region due to the large Shafranov shift. The Mercier criterion (D_I) shows that the plasma is stable all over the plasma region and consequently the low-*n* interchange modes do not appear. Although the typical SDC plasma is stable to the interchange mode, it is worthwhile to investigate the other pressure profiles and the magnetic field configurations to know the role of the MHD instabilities on the experimentally obtained SDC plasmas. In the experiment, the SDC plasmas cannot be produced in the configuration with inward shifted magnetic axis. Such configuration tends to be MHD unstable, in which the core resonant interchange modes become unstable in case of relatively low-beta plasma with finite pressure gradient in the core region. We will investigate how the MHD instabilities affect the production of the SDC plasma with steep pressure gradient in the core region in the configuration with inward shifted magnetic axis.

Keywords: Large Helical Device, MHD, Internal Diffusion Barrier,

1. Introduction

The characteristics of confinement properties and magnetohydrodynamics (MHD) stabilities of the super dense core (SDC) plasmas are intensively studied in the Large Helical Device (LHD) experiment [1]. Figure1 shows the attainable central beta β_0 against to the position of the magnetic axis R_{ax}. The SDC plasmas are produced in the outward-shifted configuration R_{ax} > 3.75[m]. On the other hand, in the inward-shifted configuration R_{ax} < 3.70[m], SDC plasmas are not obtained. The steep pressure gradient maintains at the core region for R_{ax} = 3.75m case whereas the gradual gradient appears in the inward-shifted configuration of R_{ax} = 3.6m as shown in Fig.2. We focus on stabilities of magnetohydrodynamics (MHD) of SDC plasmas in this study. MHD stabilities can be categorized into the ideal mode and resistive mode. Each mode, furthermore, can be classified into the low-*n*

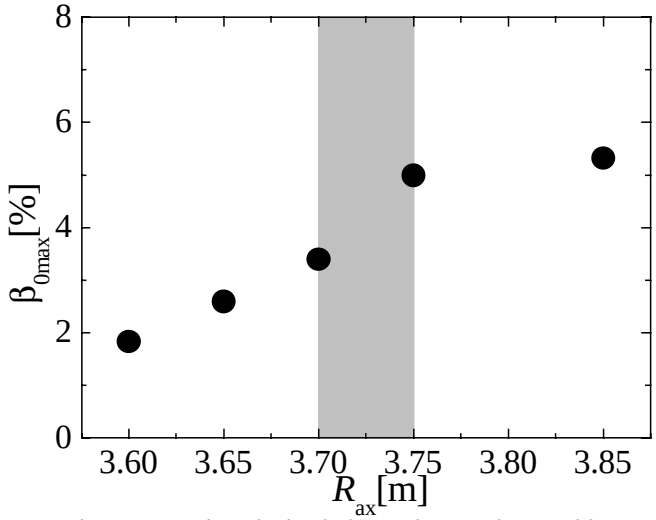

Fig.1 Magnetic axis (R_{ax}) dependence of central beta (β_0). Threshold is seen at between R_{ax} = 3.7m and 3.75m. The β_0 seems to be suppressed in inward shifted configuration (R_{ax} < 3.7).

author's e-mail:narusima@LHD.nifs.ac.jp

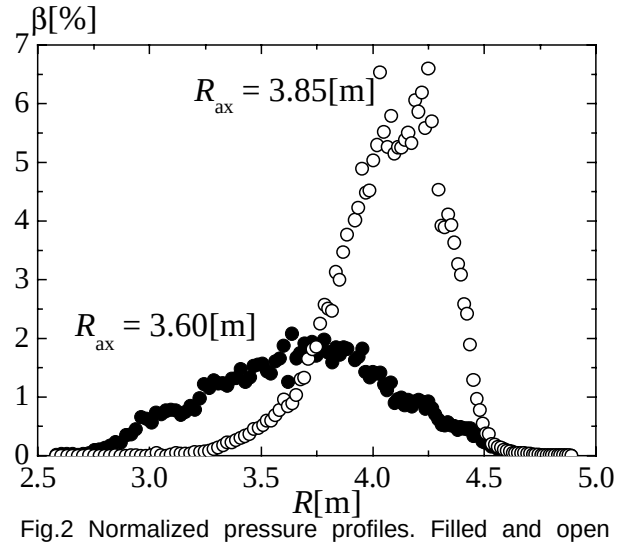

Fig.2 Normalized pressure profiles. Filled and open circles indicate the case of R_{ax} = 3.60[m] and 3.85[m] respectively. The steep gradient is seen in R_{ax} = 3.85[m].

(global) mode and high-*n* (local) mode. Here, *n* means the toroidal Fourier mode number. In this study, we have investigated about low-*n* ideal mode, high-*n* ideal mode, and resistive high-*n* mode. The latter mode relates to the plasma transport. The analyses of low-*n* ideal mode are carried out by using 3-D ideal MHD stability code TERPSICHORE [2]. The Mercier index shows the stability of ideal high-*n* mode. The resistive high-*n* mode is examined from local parameters of specific volume, Reynolds number and pressure gradient. The equilibria analyzed here are solved as the result of the HINT/HINT2 codes [3,4].

This paper is organized as follows. Characteristics of MHD stability of experimentally obtained plasmas are described in the following section. In section 3, equilibria with modeled pressure profiles are analyzed to orient the

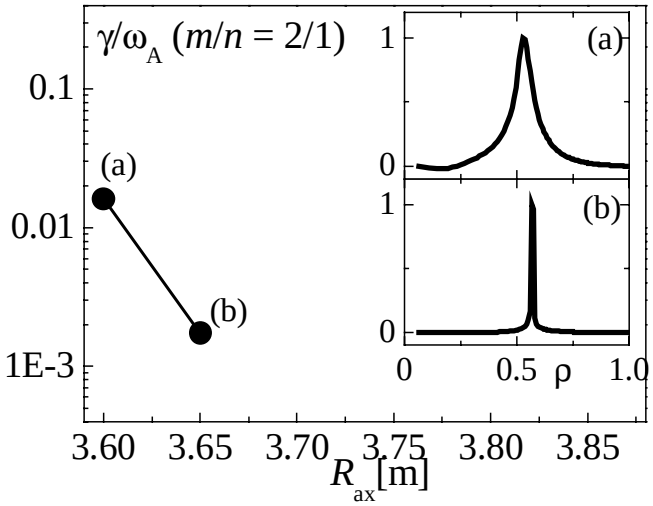

Fig.3 Dependence on the growth rate of *m*/*n* = 2/1 mode of R_{ax}. Typical mode structures in case of (a)R_{ax} = 3.6[m] and (b)R_{ax} = 3.65[m] are also shown.

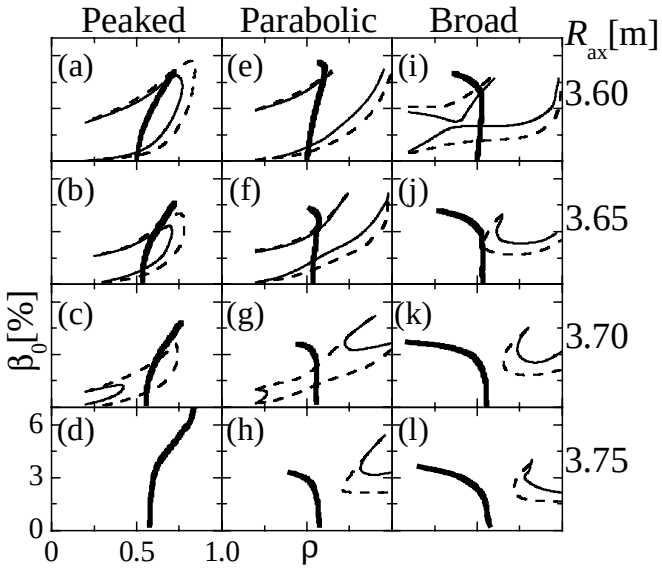

Fig.4 Contour lines of Mercier index and the position of ι/2π = 1/2 surface in ρ - β_0 space. Dashed and solid thin lines indicate D_I = 0 and 0.2 respectively. Bold solid lines correspond to the position of ι/2π = 1/2.

experimental results. Finally, we will discuss and summarize in section 4.

2. Characteristics of MHD stability of experimentally obtained plasmas

Experimentally obtained SDC plasmas have a steep pressure gradient in the core region which corresponds to around the position of the rotational transform ι/2π = 1/2. We focus on, therefore, the *m*/*n* = 2/1 mode as a low-*n* ideal MHD mode. Here, *m* means the poloidal Fourier mode number. The analyses of low-*n* ideal mode are carried out by using 3-D ideal MHD stability code TERPSICHORE. The relationship between the growth rate and R_{ax} is shown in Fig.3. In case of R_{ax} = 3.6[m], the *m*/*n* = 2/1 mode is unstable with the growth rate $\gamma/\omega_A = 1.62\times10^{-2}$ and the wide mode structure appeasers as shown in Fig.3(a). In case of R_{ax} = 3.65[m], the growth rate is 1.74×10^{-3} and the width of the structure is narrower than that in case of R_{ax} = 3.6m. It is reported that the growth rate of $\gamma/\omega_A = 10^{-2}$ is defined as the stability boundary [5]. It can be, therefore, considered that the ideal low-*n* (*m*/*n* = 2/1) interchange mode is stable except for the configuration with R_{ax} = 3.6[m].

3. MHD stability of analytical equilibrium

Equilibria with modeled pressure profiles are analyzed to orient the experimental results. Here, three kinds of pressure profiles of parabolic ($\beta = \beta_0(1 - \rho^2)(1 - \rho^8)$), peaked ($\beta = \beta_0(1 - \rho^2)^2$), and broad ($\beta = \beta_0(1 - \rho^4)(1 - \rho^8)$) are adopted. The contour lines of Mercier index D_I are shown in Fig. 4 where dashed and solid thin lines

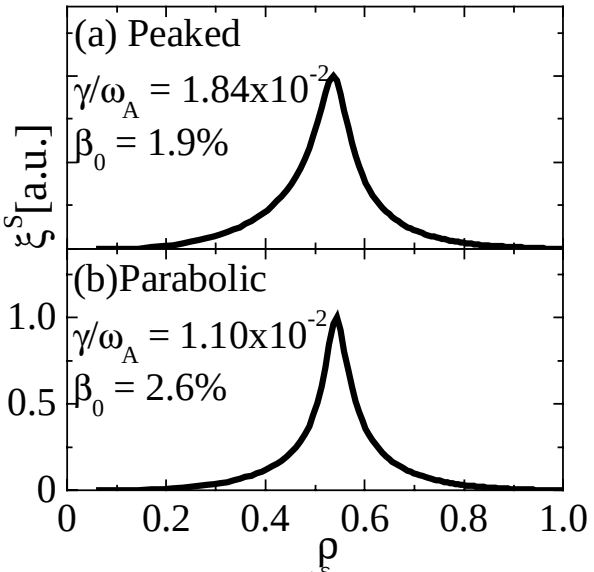

Fig.5 Typical structure of ξ^S of m/n = 2/1 mode. (a) Peaked pressure profile (b) Parabolic pressure profile.

indicate D_I = 0 and 0.2 respectively. Bold solid lines correspond to the position of $\iota/2\pi$ = 1/2. In equilibria with R_{ax} = 3.60[m] (Fig.4(a)(e)(i)), Mercier unstable regions dominate the ρ - β_0 space. Mercier unstable region generally narrows with increasing R_{ax}. In particular, the equilibrium with peaked profile in R_{ax} = 3.75[m] is Mercier stable all over the region (Fig.4(d)).

In order to investigate the global ideal mode, we have analyzed the stability of m/n = 2/1 mode which mainly resonates at core region. The low-n ideal mode tends to be unstable when the resonant surface obviously enters the Mercier unstable region. The ideal low-n interchange mode is destabilized (as above mentioned, growth rate becomes $\gamma/\omega_A > 10^{-2}$) in R_{ax} = 3.60[m] with peaked and parabolic profiles, in which the mode structures are shown in Fig.5. In each cases, (peaked (Fig.5 (a)) and parabolic Fig.5 (b)), the growth rate is γ/ω_A = 1.84x10^{-2} and 1.10x 10^{-2} respectively. The shape of mode structure is similar to each other, in which the full width at half maximum, Δρ, is Δρ ~ 0.1 and the position of the peak corresponds to around ρ = 0.54. In the other equilibria (R_{ax} >3.6[m]), the low-n mode (m/n = 2/1) does not appear.

The orientation of experimental results from the viewpoint of ideal MHD instability is shown in Fig.6. The left figure (Fig.6 (a)) shows the global ideal MHD unstable region by solid lines and the right one (Fig.6 (b)) indicates the unstable region of the local MHD mode. The experimental results of central beta β_0 are superimposed. The experimentally obtained plasmas generally locate far from the MHD unstable (m/n = 2/1 mode) region as shown in Fig.6 (a). Some of experimental results (R_{ax} = 3.6[m] and 3.65[m]), on the

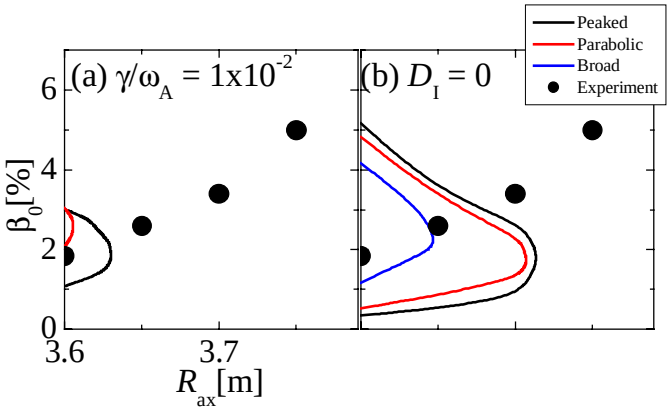

Fig.6 Ideal MHD unstable region of (a) global mode and (b) local mode. Black, red and blue solid line indicates pressure profile of peaked, parabolic and broad respectively. Closed circles shows experimental result of central beta.

other hand, enter the Mercier unstable region as shown in Fig.6(b). These results suggest that the ideal global mode does not affect the beta (gradient) in outward-shifted configuration. High-n ideal mode might influence the MHD characteristics because the unstable region of high-n ideal mode covers the region where the experimental data exists.

4. Discussion and summary

The ideal MHD stability of SDC plasma is investigated. The results show that the SDC plasmas are stable against to the ideal MHD mode. In order to investigate the other MHD stability, we will discuss the possibility of the resistive mode here. The resistive MHD instability is well correlated with the transport via the resistive pressure gradient driven turbulence. The coefficient of the particle diffusion D is defined by the magnetic curvature (κ_n), Reynolds number (S) and pressure gradient ($d\beta/d\rho$) as follows [6-7].

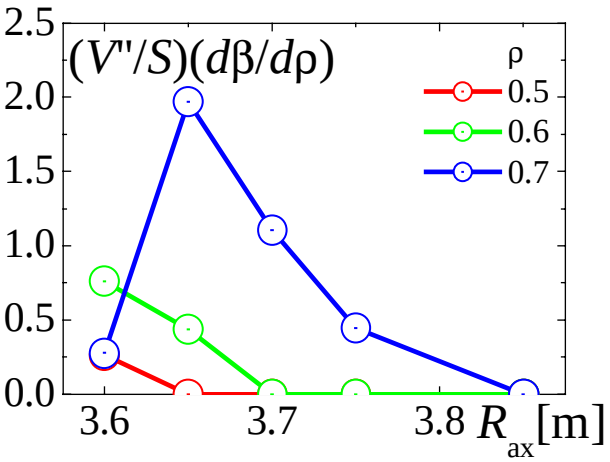

Fig.7 Qualitative behavior of diffusion by resistive pressure gradient driven turbulence.

$$D \propto \frac{\kappa_n}{S}\frac{d\beta}{d\rho} \qquad (1)$$

The qualitative behavior of the diffusion against to the R_{ax} is shown in Fig.7. The deferential of specific volume V'' is used here instead of κ_n to estimate the coefficient of the particle diffusion. The plot at $\rho = 0.7$ of $R_{ax} = 3.6$[m] indicates the small value, which comes from the local flatting of the pressure gradient. Figure 7 shows that the diffusion by the resistive pressure gradient driven turbulence generally continuously decreases with the R_{ax}. The diffusion at $\rho = 0.5$ and 0.6, in particular, goes to zero around $R_{ax} = 3.7$[m] where the threshold is seen as shown in Fig.1. In other word, diffusion tends to become large in the inward-shifted configuration. Further analyses about resistive mode are required.

Acknowledgement

This study was supported by a Grant-in-Aid for Scientific Research (A)(No.17206094) from the Ministry of Education, Culture, Sports, Science and Technology of Japan. This work was supported by NIFS under Contract No.NIFS07ULPP535.

References

[1] N. Ohyabu *et al* Phys. Rev. Lett. **97**,055002(2006)
[2] W.A. Cooper Plasma Phys. Control. Fusion **34**, 1011 (1992)
[3] K. Harafuji *et al* J. Comput. Phys. **81** 169 (1989)
[4] Y. Suzuki *et al* Nucl. Fusion **46** L19 (2006)
[5] K. Y. Watanabe *et al* Fusion Sci. Technol. **46** 24 (2004)
[6] B.A. Carreras et al. Phys. Fluids **30**,1388(1987)
[7] B.A. Carreras et al. Phys. Fluids B1,1011(1989)